Adipose-specific peroxisome proliferator-activated receptor γ knockout causes insulin resistance in fat and liver but not in muscle

Weimin He*†, Yaacov Barak†‡§, Andrea Hevener*†, Peter Olson§¶, Debbie Liao§, Jamie Le*, Michael Nelson§, Estelita Ong§, Jerrold M. Olefsky*‖, and Ronald M. Evans§‖**

Departments of *Medicine and ¶Biology, University of California at San Diego, La Jolla, CA 92093; ‡The Jackson Laboratory, Bar Harbor, ME 04609; and §Gene Expression Laboratory and **Howard Hughes Medical Institute, The Salk Institute, La Jolla, CA 92037

Contributed by Ronald M. Evans, October 22, 2003

Syndrome X, typified by obesity, insulin resistance (IR), dyslipidemia, and other metabolic abnormalities, is responsive to antidiabetic thiazolidinediones (TZDs). Peroxisome proliferator-activated receptor (PPAR) γ, a target of TZDs, is expressed abundantly in adipocytes, suggesting an important role for this tissue in the etiology and treatment of IR. Targeted deletion of PPARγ in adipose tissue resulted in marked adipocyte hypocellularity and hypertrophy, elevated levels of plasma free fatty acids and triglyceride, and decreased levels of plasma leptin and ACRP30. In addition, increased hepatic glucogenesis and IR were observed. Despite these defects, blood glucose, glucose and insulin tolerance, and insulin-stimulated muscle glucose uptake were all comparable to those of control mice. However, targeted mice were significantly more susceptible to high-fat diet-induced steatosis, hyperinsulinemia, and IR. Surprisingly, TZD treatment effectively reversed liver IR, whereas it failed to lower plasma free fatty acids. These results suggest that syndrome X may be comprised of separable PPARγ-dependent components whose origins and therapeutic sites may reside in distinct tissues.

syndrome X

Obesity, insulin resistance (IR), hyperlipidemia, and hypertension, collectively called the metabolic syndrome or syndrome X, occur at an alarming frequency in Western cultures. Peroxisome proliferator-activated receptor (PPAR) γ is considered a portal to syndrome X because adipose tissue expresses high levels of PPARγ, and obesity is a primary risk factor for the disease. Accordingly, an understanding of the molecular and cellular basis of this syndrome can be approached by analyzing the role of PPARγ in the generation and treatment of this disorder. Importantly, IR is typified by reduced sensitivity to insulin in skeletal muscle, and this defect is a preclinical symptom in subjects destined to develop type II diabetes.

Previous studies have shown that PPARγ functions as a central transcriptional regulator of both adipogenic and lipogenic programs (1). PPARγ is also implicated in whole-body glucose homeostasis and insulin sensitivity. Thus, point mutations in the ligand-binding domain of PPARγ result in diabetes and hypertension in humans (2). The involvement of PPARγ in systemic insulin sensitization is further supported by the fact that thiazolidinediones (TZDs), a class of antidiabetic agents, are high-affinity PPARγ ligands (3). These drugs enhance adipocyte differentiation (4, 5) and ameliorate IR (6, 7).

TZD-induced insulin sensitization is manifested by increased insulin-stimulated glucose uptake mainly in skeletal muscle, the major tissue for glucose disposal (8). Compared to its robust expression in adipose tissue, however, PPARγ is barely detectable in muscle. It is therefore unclear whether TZD acts directly in skeletal muscle or indirectly through the activity of fat PPARγ. Lines of evidence support the involvement of adipose tissue in systemic insulin sensitivity. Diet and genetically induced obesity are closely associated with hyperinsulinemia and IR (9). A polymorphism of PPARγ2, Pro12Ala, which decreases receptor activity, is related with lower body mass index and enhanced insulin sensitivity in humans (10), and this beneficial effect of partially blunted PPARγ activity is recapitulated in more insulin-sensitive heterozygous PPARγ mice (11, 12). These data support roles of fat PPARγ in the development of IR. However, IR in lipodystrophic humans and animals suggests an essential role of fat PPARγ for systemic insulin sensitivity (13–15). Indeed, transplantation of wild-type (wt) adipose tissue into fatless A-ZIP/F1 mice unresponsive to TZD treatment (16) led to lower plasma glucose and insulin levels (17). These seemingly inconsistent findings raise the question of what roles fat PPARγ plays in insulin sensitivity and whether it mediates the effects of TZD action in mature adipocytes.

To address these questions, we used the Cre-*loxP* system (18) to generate mice deficient in PPARγ only in fat. Our study reveals that PPARγ is essential for the long-term survival and homeostatic function of the adipocyte and that its deficiency causes substantial fat cell loss and compensatory hypertrophy. The fat PPARγ-deficient (FKOγ) mice exhibit increased plasma free fatty acids (FFAs) and triglyceride (TG), decreased leptin and Acrp30 levels, fatty liver, and enhanced hepatic gluconeogenesis. However, these mice do not develop muscle IR unless placed on a high-fat diet (HFD), suggesting that components of syndrome X may arise independent of each other, with the disease representing an aggregate of phenotypes.

Materials and Methods

Generation of PPARγ^{loxP} and aP2-Cre Mice. A single *loxP* site and a *neo* cassette flanked by two additional *loxP* sites were introduced into the introns upstream and downstream of exons 1 and 2 (Fig. 1*A*). G418-selected, homologously recombined embryonic stem (ES) cells were confirmed by Southern analysis (Fig. 1*B*), correctly targeted clones were transfected with Cre expression plasmid, and floxed clones were identified by Southern analysis (Fig. 1 *A* and *C*). Chimeras with germ-line transmission were obtained, and the presence of the floxed allele in offspring was confirmed by PCR. For fat-specific Cre-transgenic mice, a 5.4-kb aP2 gene promoter was used to drive Cre cDNA expression. The transgene was microinjected into pronuclei, and its transmission into progeny was assessed by PCR.

PCR genotyping was carried out by using the following

Abbreviations: IR, insulin resistance; PPAR, peroxisome proliferator-activated receptor; TZD, thiazolidinedione; FFA, free fatty acid; FKOγ, fat PPARγ-deficient; HFD, high-fat diet; BAT, brown adipose tissues; WAT, white adipose tissues; CCAAT enhancer-binding protein; HGP, hepatic glucose production; wt, wild type; ES, embryonic stem; KO, knockout.

†W.H., Y.B., and A.H. contributed equally to this work.

‖To whom correspondence may be addressed at: (J.M.O.) Department of Medicine, University of California at San Diego, La Jolla, CA 92093. E-mail: jolefsky@ucsd.edu. (R.M.E.) The Salk Institute/Howard Hughes Medical Institute, 10010 North Torrey Pines Road, La Jolla, CA 92037. E-mail: evans@salk.edu.

www.pnas.org/cgi/doi/10.1073/pnas.2536828100

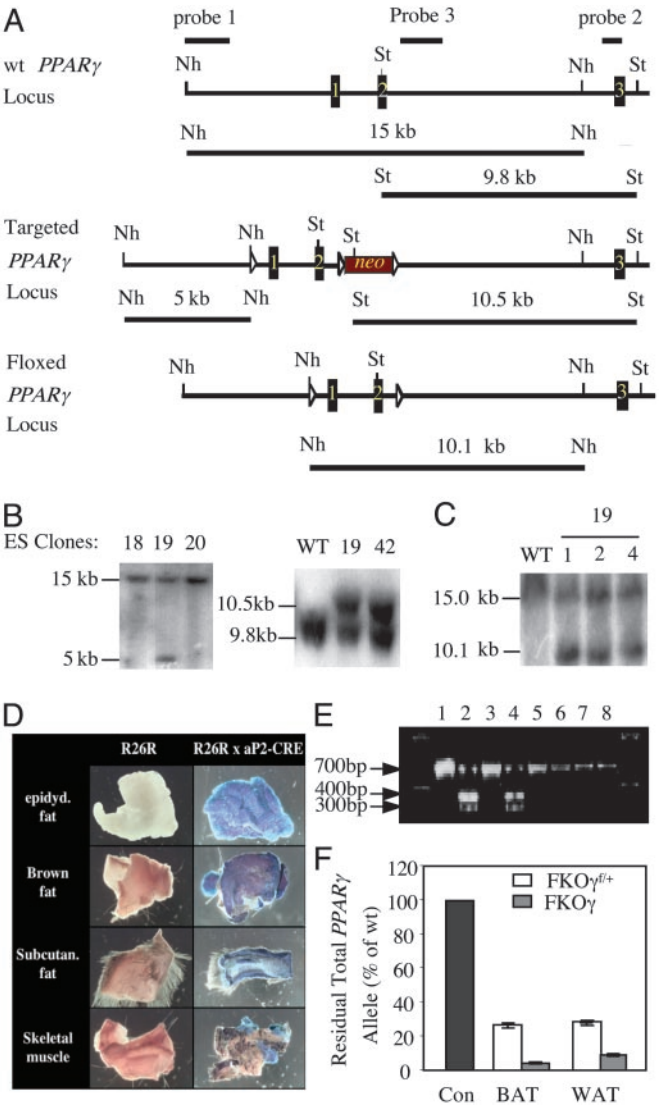

Fig. 1. PPARγ targeting strategy and aP2-Cre transgene activity. (*A*) Shown (top to bottom) are the wt, targeted, and floxed *pparγ* gene loci. Probes 1–3 were used to identify recombinants. Sizes and positions of detectable restricted fragments are shown. (*B*) Southern analysis of targeted ES cells. (*Left*) Hybridization with 5′ probes. (*Right*) Hybridization with 3′ probes (*C*) Southern blot with probe 3 of ES cells transiently transfected with a Cre plasmid. (*D*) 5-Bromo-4-chloro-3-indolyl β-D-galactoside staining of BAT, WAT, skin, and skeletal muscle from ROSA26 Con and ROSA/aP2-Cre mice. (*E*) Detection of wt and mutant PPARγ1 mRNA by RT-PCR. Lane 1, wt BAT; lane 2, FKO BAT; lane 3, wt WAT; lane 4, FKO WAT; lanes 5–8, FKO macrophages, heart, skeletal muscle, and liver, respectively. Arrows indicate the wt (700-bp) and mutant (300- and 400-bp) PCR products. (*F*) Southern blot of DNA from BAT and WAT of FKO$\gamma^{fl/+}$ and FKO$\gamma^{f/f}$. Recombination efficiencies are depicted as residual total PPARγ allele relative to wt.

primers: for the Cre transgene, 5′-GCATTACCGGTCGATGCAACGAGTG-3′ and 5′-GAACGCTAGAGCCTGTTTTGCACGTTC-3′; and for the upstream loxP site, 5′-CTAGTGAAGTATACTATACTCTGTGCAGCC-3′ and 5′-GTGTCATAATAAACATGGGAGCATAGAAGC-3′. Genomic DNA was amplified by 35 cycles of 94°C for 20 s, 60°C for 30 s, and 72°C for 55 s.

Southern/Northern Analyses and RT-PCR. Southern analysis of genomic DNA isolated from ES cells and various mouse tissues was performed by using ^{32}P-labeled probes (High Prime DNA Labeling Kit, Roche Molecular Biochemicals). Northern blot analyses were performed on total RNA isolated from mouse tissues by using TRIzol (Invitrogen). Reverse transcription was performed with SuperScript (Invitrogen). Sense (5′-GTCACGTTCTGACAGGACTGTGTGAC-3′) and antisense (5′-TATCACTGGAGATCTCCGCCAACAGC-3′) primers were designed to anneal to regions in exons A1 and 4 of PPARγ1, respectively, which distinguish the full-length (700-bp) and recombined (300-bp) transcripts. PCR was performed by 40 cycles of 94°C for 20 s, 60°C for 30 s, and 72°C for 60 s.

Histochemistry. Tissues were fixed in Bouins' buffer and paraffin-embedded. Sections were subjected to standard hematoxylin/eosin staining. For oil red O staining, livers were embedded in OCT and cryosectioned. For 5-bromo-4-chloro-3-indolyl β-D-galactoside staining, tissues were fixed in 4% paraformaldehyde for 3 h at 4°C before staining at 37°C overnight.

HFD Feeding and TZD Treatment. Adult mice were fed a HFD (40% calories from fat; Bioserv, Frenchtown, NJ) for 5 weeks. For TZD treatment, customized rosiglitazone-containing chow diet (Harlan Laboratories, Haslett, MI) was fed to mice at a concentration of 3 mg/kg per day.

Glucose and Insulin Tolerance Tests and Hyperinsulinemic–Euglycemic Clamp. For glucose or insulin tolerance tests, animals were fasted for 6 h and a basal blood sample was taken, followed by i.p. injection of glucose (1,000 mg/kg; Abbott) or insulin (0.85 units/kg; Novolin R, Novo-Nordisk, Copenhagen). Blood samples were drawn at 15, 30, and 60 min or at 15, 30, 45, 60, 90, and 120 min after the injection. Mouse clamping studies were performed as described in ref. 18.

Results

Adipose-Specific PPARγ Gene Targeting. To uncover the function of PPARγ in mature adipocytes and its linkage to syndrome X-associated defects, *loxP* sites were introduced on either side of the exons 1 and 2 of PPARγ to generate floxed PPARγ mice (Fig. 1 *A–C*). Cre-mediated deletion of these exons is predicted to result in loss of PPARγ1 and a nonfunctional, N-terminal, 43-aa translational product of PPARγ2 that misses the partial AF1 domain and the first zinc finger of the DNA binding domain (19).

Fat-specific Cre expression was achieved by placing Cre cDNA under the control of the 5.4-kb promoter fragment of the *ap2* gene (aP2-Cre). Because aP2 is a downstream target of PPARγ (1), this strategy is expected to delete PPARγ after formation of fat depots, allowing normal differentiation of adipocytes. A founder line exhibiting strong Cre expression in both brown adipose tissues (BAT) and white adipose tissues (WAT) was expanded and used in this study (see also ref. 20). The tissue specificity and efficiency of this Cre transgene were confirmed by breeding with the ROSA R26R reporter mouse (21), where aP2-Cre directed a virtually complete recombination and activation of β-gal expression in gonadal, brown, and s.c. adipose depots, but not in skeletal muscle (Fig. 1*D*). In PPARγ$^{f/f}$/aP2-Cre mice, RT-PCR detects recombinant PPARγ only in adipose tissue and not in liver, heart, skeletal muscle, or macrophages (Fig. 1*E*), demonstrating the general utility of this aP2-Cre-transgenic line for adipocyte-specific recombination.

Floxed PPARγ (PPARγ$^{f/+}$) mice were crossed to aP2-Cre mice to generate PPARγ$^{f/+}$/Cre progeny. These were then backcrossed for four generations against C57BL/6J mice. The backcrossed PPARγ$^{f/+}$/Cre mice were subsequently interbred to yield six derivative strains: (*i*) PPARγ$^{f/f}$ (con), (*ii*) PPARγ$^{f/f}$/Cre (FKOγ), (*iii*) PPARγ$^{f/+}$ (con$^{f/+}$), (*iv*) PPARγ$^{f/+}$/Cre (FKOγ$^{f/+}$), (*v*) PPARγ$^{+/+}$ (wt), and (*vi*) PPARγ$^{+/+}$/Cre (Cre). Mice from all strains were born at predicted Mendelian frequencies, ap-

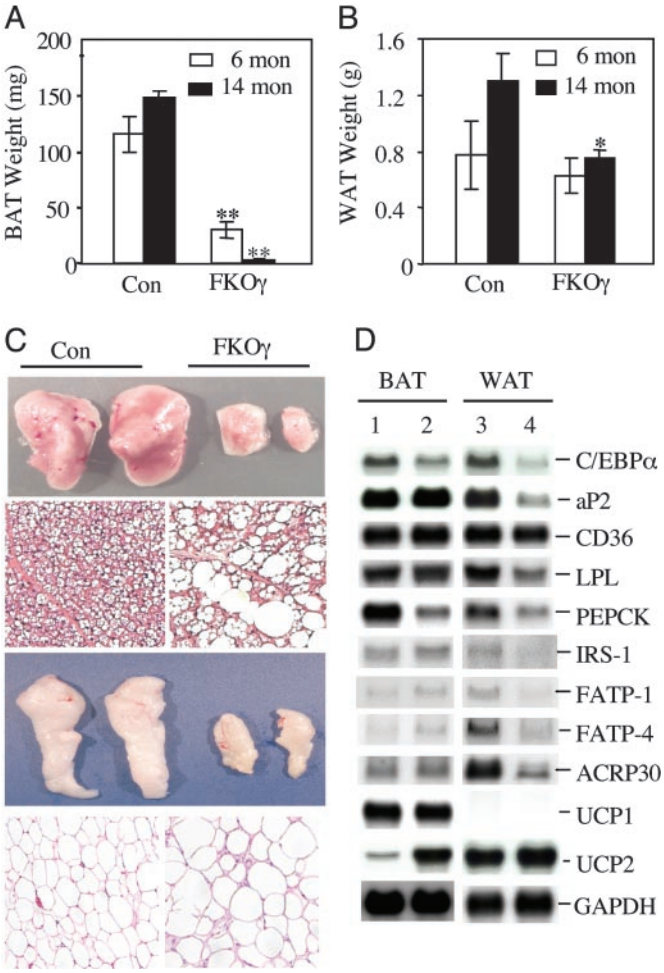

Fig. 2. Deletion of PPARγ in fat leads to progressive lipodystrophy. BAT (*A*) and WAT (*B*) weight changes in 6- and 14-month-old Con and FKOγ mice. Values are the mean ± SEM ($n = 10$). (*C*) Gross morphology and histology of BAT (top two panels) and WAT (bottom two panels) from 6-month-old Con and FKOγ mice. (*D*) Northern blot analysis of adipocyte genes in BAT and WAT in Con (lanes 1 and 3) and FKOγ (lanes 2 and 4) mice. Total RNA from each group ($n = 5$) was pooled, and 10 μg of RNA per group was analyzed.

peared grossly normal, and produced normal progeny. No weight differences were observed among all six strains during the first 6 months of life, regardless of their floxed or Cre allele combination.

To examine the recombination efficiency of FKOγ mice, genomic DNA isolated from BAT and WAT was subjected to Southern analysis. As controls, FKO$\gamma^{f/+}$ mice revealed an ≈35% recombination of PPARγ in both WAT and BAT (Fig. 1*F*), corresponding to 70% of all cells in these depots. Given that ≈ 30% of cells in adipose tissue are nonfat cells (ref. 22 and data not shown), this reflects close to 100% recombination efficiency in the adipocyte population, indicating a high efficacy of the Cre, confirming the high efficacy of the Cre transgene. In FKOγ mice, the dramatic reduction in adipose cellularity (Fig. 2*A*; see below), and a recombination rate of 55% and 45% in the residual BAT and WAT pads, respectively, combine to reflect >95% and ≈90% loss of the initial PPARγ.

Progressive Lipodystrophy in PPARγ-Deficient BAT and WAT. Although FKOγ mice gained similar weight during the first 6 months of life (data not shown), they nevertheless showed striking morphologic defects when they were young; 4- to 6-week-old FKOγ mice already displayed marked diminution of the interscapular fat pads, and by 6 months BAT mass was reduced by >70% (Fig. 2 *A* and *C*). The mutant BAT displayed signs of inflammation, including monocyte infiltration and fibrosis. More importantly, whereas wt brown adipocytes were uniformly polygonal, with multilocular cytoplasmic vacuoles and central nuclei, cells from FKOγ mice were much larger and vastly variable in size, displaying either large multilocular vacuoles or a white adipocyte-like large unilocular droplet (Fig. 2*C*). The 3- to 4-fold increase in cell diameter reflects a >30-fold increase in volume, indicating a reduction of >95% of fat cells.

WAT underwent similar changes but progressed at differing rates. s.c. adipocytes were lost very early (data not shown), whereas epididymal fat maintained normal mass up to 6 months (Fig. 2*B*). Nevertheless, fibrosis and macrophage infiltration were evident, and >50% of white adipocytes were highly hypertrophic (Fig. 2*C*), implying a >80% loss of adipocytes. Very small, likely nascent adipocytes were observed, especially in aged mice. Thus, PPARγ is essential for postdifferentiation survival of brown and white adipocytes, and its inactivation results in fat cell loss, compensatory hypertrophy, and new fat cell differentiation.

We next examined the effect of PPARγ deletion on the expression of adipocyte genes from residual surviving tissue (Fig. 2*D*). Multiple genes were down-regulated in FKOγ WAT including those involved in lipogenesis, fatty acid uptake, and storage, such as CCAAT enhancer-binding protein α, aP2, lipoprotein lipase, phospho*enol*pyruvate carboxykinase, and fatty acid transporters 1 and 4. In addition, the insulin receptor substrate IRS-1 and ACRP30 were also decreased, indicating a marked compromise in the function of mutant WAT. Whereas phospho*enol*pyruvate carboxykinase and CCAAT enhancer-binding protein α were also down-regulated in BAT, all other tested genes were unchanged. Surprisingly, expression of the BAT-specific uncoupling protein gene UCP-1, reported previously to be regulated by PPARγ (23), was unchanged in mutant BAT, whereas UCP-2 was up-regulated. Overall, the differences in gene expression profiles between BAT and WAT of FKOγ mice suggest that PPARγ has both unique and partially overlapping functions in these two forms of fat. It also indicates that some genes, once activated, do not depend on continued PPARγ expression.

Metabolic Assessment of FKOγ Mice. Metabolic parameters of FKOγ mice were examined in the basal fasting state and during a hyperinsulinemic–euglycemic clamp. Consistent with WAT lipoatrophy, circulating levels of leptin and ACRP30 were reduced by 60% and 80%, respectively, in FKOγ mice compared to control (Con) animals (Table 1). In contrast, basal plasma FFAs were 80% and 20% higher in 6- and 14-month-old FKOγ mice, respectively (Fig. 3*A* and Table 1), and blood TG levels were also elevated (Table 1). During the clamp, insulin reduced FFA levels in both Con and FKOγ mice. However, plasma FFAs remained significantly higher in both young and old FKOγ mice (3-fold and ≈35%, respectively), indicative of primary IR in adipocytes.

Surprisingly, glucose tolerance in FKOγ mice did not differ from that of Con animals, with insulin tolerance tests revealing comparable insulin-stimulated glucose uptake in FKOγ and Con mice (Fig. 3 *B* and *C*). This indicates that systemic insulin sensitivity was maintained. Consistent with these data, fasting blood glucose and insulin levels in FKOγ mice were comparable to Con mice (Table 1). Clamp studies showed relatively normal insulin-stimulated muscle glucose disposal rate in 14-month-old FKOγ mice (Fig. 3*D*), further supporting the conclusion that muscle insulin sensitivity in knockout (KO) mice is largely intact.

Table 1. Metabolic parameters of 14-month-old FKOγ mice

Genotype	Con	FKOγ
Blood glucose, mg/dl		
Basal	137 ± 5.6	125 ± 5.4
Clamp	148 ± 1.9	148 ± 0.96
Blood insulin, ng/ml		
Basal	0.87 ± 0.02	0.82 ± 0.25
Clamp	9.4 ± 0.6	10.3 ± 0.6
FFA (mmol/l)		
Basal	0.82 ± 0.09	0.99 ± 0.05
Clamp	0.43 ± 0.02*	0.58 ± 0.06*#
Blood triglyceride, mg/dl	122.8 ± 15	151 ± 19
Leptin, ng/ml	3.76 ± 1.0	1.5 ± 0.33#
Acrp30, mg/ml	20.9 ± 2.2	3.9 ± 0.72#
Muscular TG, μmol/g of tissue	5.7 ± 2.0	7.6 ± 3.1
Liver TG, μmol/g of tissue	6.3 ± 2.0	11.7 ± 4.2#

Data represent the mean ± SEM ($n = 8$). Blood was obtained from the Con and FKOγ mice before and during clamping study. *, $P < 0.05$, basal vs. clamping; #, $P < 0.05$, Con vs. FKOγ.

Steatosis and Hepatic IR. Lipodystrophy is often accompanied by a fatty liver (14, 15); therefore, we examined livers from FKOγ mice. Whereas liver weight and gross morphology from 6-month-old FKOγ mice were similar to those of Con animals (Fig. 4*A*), numerous lipid-laden vacuoles in hepatocytes revealed that these livers are already steatotic (Fig. 4*B*). When aged further, these mice developed marked hepatomegaly, and steatosis was exacerbated further (Fig. 4*A*).

Hepatic glucose production (HGP) was elevated in FKOγ mice. Although insulin still suppressed glucose production in KO animals during clamping, this inhibition was not as effective as in Con mice (Fig. 4*C*), indicating the presence of hepatic IR in FKOγ mice.

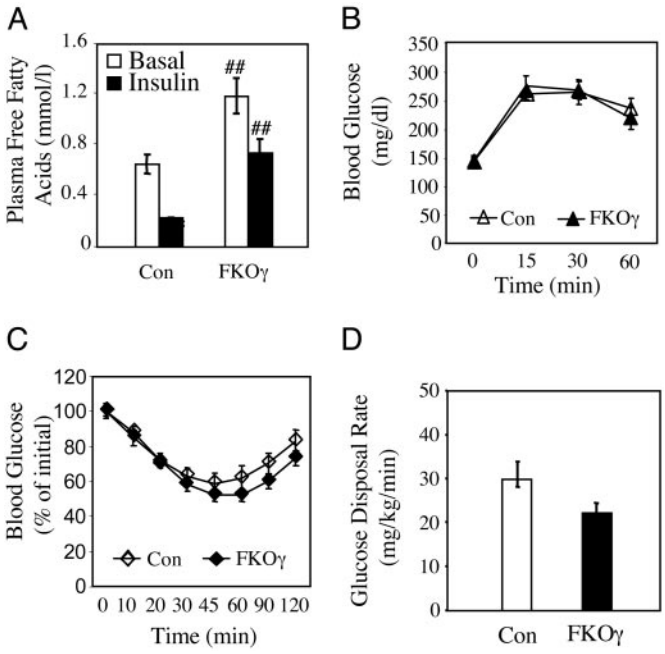

Fig. 3. FKOγ mice show relatively normal insulin sensitivity. (*A*) Blood FFA levels in basal state and during clamp. Values from each group are the mean ± SEM ($n = 8$). *, $P < 0.05$, basal vs. clamp; ##, $P < 0.01$, FKOγ vs. Con. Glucose tolerance (*B*) and insulin tolerance (*C*) tests in Con and FKOγ mice. Values are the mean ± SEM ($n = 10$). (*D*) Insulin-stimulated muscle glucose uptake during clamp. Values are the mean ± SEM ($n = 8$).

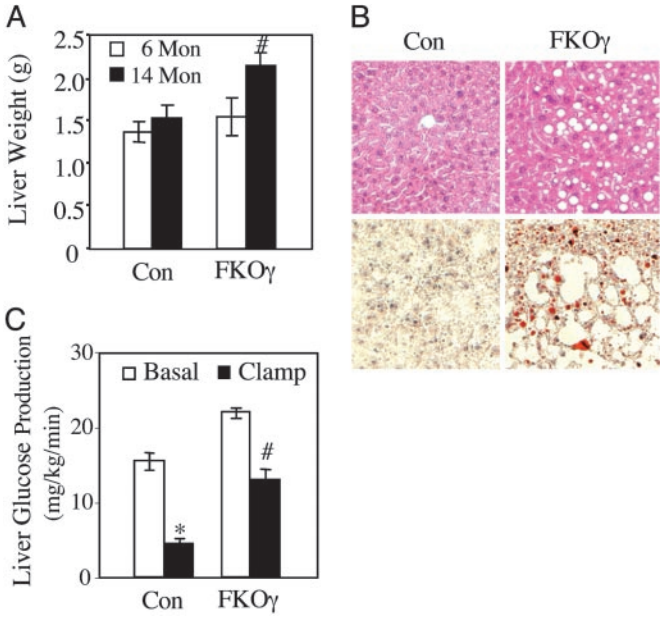

Fig. 4. Fatty liver and hepatic IR. (*A*) Liver weights from 6- and 14-month-old Con and FKOγ mice. #, $P < 0.05$. (*B*) Histology (*Upper*) and oil red O staining (*Lower*) of livers from 6-month-old Con and FKOγ mice. (*C*) HGP in basal state and during clamp study. *, $P < 0.05$, basal vs. clamp; #, $P < 0.05$, FKOγ vs. Con during clamp.

Effects of a HFD on FKOγ Mice. Four weeks of high-fat feeding increased the body weight of Con mice by >30% (Fig. 5*A*), primarily by enlarging BAT and WAT (Fig. 5*B*). In contrast, FKOγ mice gained significantly less weight, and their residual BAT and WAT became more lipoatrophic, similar to the changes in older, normal diet-fed KO animals (Fig. 5*C*).

Interestingly, high-fat feeding caused a comparable 2-fold increase in fasting glycemia in both Con and FKOγ mice. However, insulin levels were 2-fold higher in FKOγ mice, suggesting that these mice are more susceptible to HFD-induced IR than are Con mice (Fig. 5 *D* and *E*). Indeed, insulin was less efficient in lowering glucose in FKOγ mice (Fig. 5*F*). Thus, adipocyte PPARγ is important for insulin sensitivity in the high-fat-fed state.

Effects of TZD Treatment in FKOγ Mice. To determine the site of TZD action, we subjected Con and FKOγ mice to 4 weeks of rosiglitazone treatment and conducted clamp studies. TZD treatment led to a comparable 15–20% increase in insulin-stimulated muscle glucose disposal rate in both Con and FKOγ mice (Fig. 6*A*). TZD treatment also lowered plasma FFAs in Con mice, yet no such effect was observed in FKOγ mice (Fig. 6*B*). This finding provides strong genetic evidence that changes in FFA levels arise directly from increased lipolysis in adipose tissue, which becomes refractory to TZD action as a result of the targeted deletion of PPARγ. In contrast, hepatic IR of FKOγ mice was almost completely normalized by TZD administration (Fig. 6*C*), suggesting that this effect is not mediated by adipocytes.

Discussion

FKOγ mice display phenotypes of progressive fat cell loss, hypertrophy of viable cells, hyperlipidemia, reduction of circulating leptin and ACRP30, fatty liver, and hepatic IR. TZD treatment failed to improve fat insulin sensitivity but normalized liver IR and improved muscle glucose disposal rate in FKOγ mice comparable with that in Con mice. These results

GENETICS

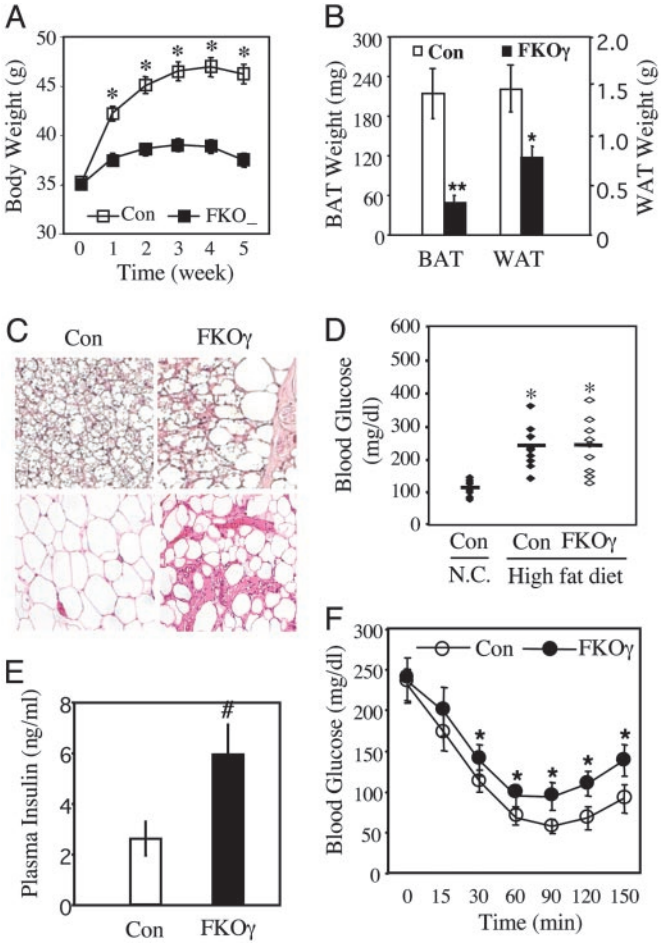

Fig. 5. HFD leads to expedited lipodystrophy and severe IR in FKOγ mice. (*A* and *B*) Body weight gain and fat pad mass change of HFD-fed Con and FKOγ mice. Values are the mean ± SEM ($n = 10$). *, $P < 0.05$. (*C*) Histology of BAT (*Upper*) and WAT (*Lower*) from Con and FKOγ mice. Fasting blood glucose (*D*) and insulin (*E*) levels in HFD-fed animals are shown. HFD causes similar elevation of fasting blood glucose levels but higher levels of insulin in FKOγ mice. Values are the mean ± SEM ($n = 10$). *, $P < 0.05$, FKOγ vs. Con. (*F*) Insulin tolerance test after HFD feeding. Values are the mean ± SEM ($n = 10$). *, $P < 0.05$, FKOγ vs. Con.

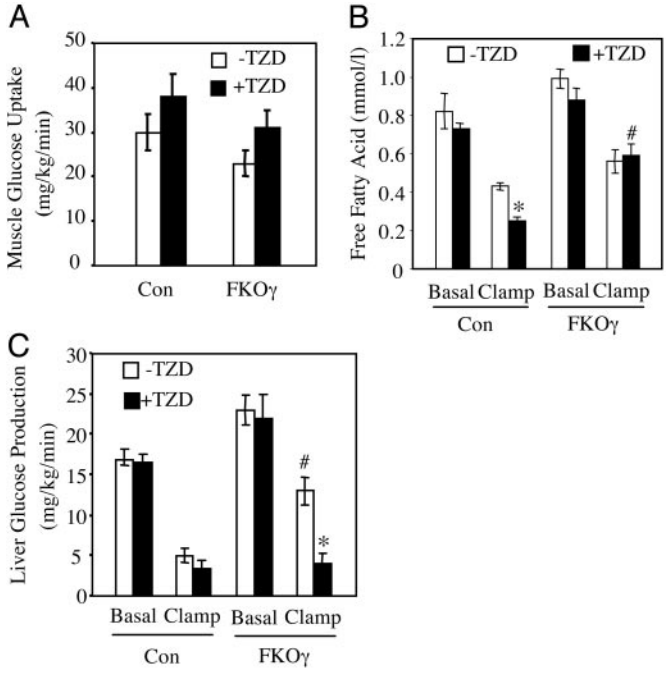

Fig. 6. TZD treatment sensitizes insulin action in muscle and liver but not in fat. (*A*) Insulin-stimulated muscle glucose disposal rate in TZD-treated and untreated FKOγ and Con mice ($n = 8$). (*B*) Antilipolytic activity of insulin in TZD-treated and nontreated Con and FKOγ mice ($n = 8$). *, $P < 0.01$, treated vs. untreated Con during clamp. #, $P < 0.01$, treated FKOγ vs. treated Con during clamp. (*C*) HGP in TZD-treated and nontreated Con and FKOγ mice ($n = 8$) in basal state and during clamp study. #, $P < 0.01$, untreated FKOγ vs. untreated Con during clamp. *, $P < 0.01$, treated and untreated FKOγ during clamp.

demonstrate the importance of fat PPARγ in maintaining normal adipocyte viability and fat and liver insulin sensitivity and suggest that syndrome X is a mosaic of components derived from distinct primary and secondary tissues with differing therapeutic capacities.

PPARγ and Adipocyte Viability and Function. Genetic studies of the function of PPARγ have been hampered by the inability of *PPARγ*-null mice to generate adipocytes (24). Our current genetic configuration bypasses this roadblock by deleting the *PPARγ* only after adipogenesis has occurred. The reduction in fat mass and subsequent progressive lipodystrophy in KO mice indicate that, in addition to the previously established critical role in adipogenesis, PPARγ also plays a genetically distinct role in maintaining the survival of the mature adipocytes. In addition, the animals become hyperlipidemic and manifest fat IR as insulin action on lipolysis is blunted. Moreover, TZD treatment fails to alleviate IR in PPARγ-deficient fat.

The reduced viability of *PPARγ*-null adipocytes leads to dramatic hypertrophy of the remaining cells and the appearance of a population of small adipocyte-like cells. We speculate that hypertrophic cells accumulate excessive amounts of lipid as compensation and that these cells ultimately are more susceptible to apoptosis. This may explain the presence of inflammation such as macrophage infiltration and fibrosis in adipose tissues of KO mice. The appearance of the small adipocyte-like cells in aged (2-year-old) KO mice strongly suggests the presence of adipocyte stem cells or a preadipocyte pool that can undergo differentiation throughout life. Whether this speculation is correct or not, severe and continuous adipose hypoplasia demonstrates that, despite compensatory mechanisms, cell loss ultimately outpaces replenishment, leading to eventual adipose failure.

Besides its requirement for viability of adipocytes, PPARγ is obviously essential for the normal function of fat cells. PPARγ regulates a number of genes involved in lipid uptake and storage in adipose tissue. Therefore, it is logical to assume that the absence of PPARγ favors lipolysis, thus impairing the antilipolytic effects of insulin. Indeed, blood FFAs are elevated, and the antilipolytic activity of insulin is severely compromised. This hypothesis is further supported by the fact that younger KO mice have higher levels of plasma FFAs, presumably because of the presence of more *PPARγ*-null adipocytes.

PPARγ and Liver Function. Deficiency of adipose PPARγ elicits dramatic secondary liver phenotypes, such as fatty liver, increased gluconeogenesis, and decreased response to insulin action on HGP. Because lipid accumulation has been shown to be related to liver IR (25, 26), it is reasonable that hyperlipidemia in FKOγ mice has a similar effect. In addition, marked reduction of adipocyte secreted factor ACRP30 could also contribute to IR, because ACRP30 is known to promote hepatic insulin

sensitivity by activating fatty acid oxidation and inhibiting phospho*enol*pyruvate carboxykinase expression (27, 28).

Interestingly, the impairment of insulin suppression on HGP was dramatically improved by TZD in FKOγ mice. This finding raises the question of where the sites of TZD action are in these mice. Because fat is PPARγ-deficient and fails to respond to TZD treatment, the sensitization effects most likely occur as a direct activation of PPARγ within the liver itself.

PPARγ and Muscle Insulin Sensitivity. Previous fatless and lipodystrophic animal models show systemic IR and diabetes (14, 15), demonstrating the importance of adipose tissue in maintaining muscle insulin sensitivity. Given that heterozygous PPARγ mice and young FKOγ mice show increased systemic insulin sensitivity (refs. 11 and 12 and data not shown), the lack of muscle IR in FKOγ mice suggests that it is adipose tissue itself, rather than fat PPARγ, that plays an important part in maintaining systemic insulin sensitivity.

It is commonly believed that accumulation of TG in muscle causes muscle IR. This concept is supported by the finding that elderly people have higher levels of TG in muscle, which leads to compromised mitochondrial function (26). The absence of muscle IR in FKOγ mice, which show elevated TG deposition in muscle, suggests that this is not necessarily the case and that the IR seen in obese subjects could also be related to factors other than ectopic fat accumulation in muscle. However, because TG accumulation in muscle of FKOγ mice is not as significant as in livers, we cannot exclude the possibility that there is a threshold above which muscle IR will surely develop.

Whereas TZD improves hyperlipidemia, it has no effect on IR and diabetes in fatless A-ZIP/F-1 mice. However, transplantation of wt adipose tissue helps to improve insulin sensitivity in these mice (17), suggesting adipocyte-related function in systemic insulin sensitivity. Adipocyte-secreted factor ACRP30 has been shown to enhance muscle insulin sensitivity (29), and TZD treatment of adipocytes up-regulates the expression of ACRP30 (30). Because FKOγ mice show a dramatic reduction of ACRP30 and develop hepatic but not muscle IR, additional adipose-derived factors may exist that are important for *in vivo* glucose homeostasis and systemic insulin sensitivity and may be TZD targets.

In summary, we show here that the loss of fat PPARγ results in progressive lipodystrophy, steatosis, and IR in fat and liver but not in muscle. These observations clearly implicate primary defects of PPARγ in fat in the generation of specific syndrome X components. We believe the human disorder is likely to be a consequence of a series of primary, secondary, and tertiary defects in key metabolic tissues. We anticipate that elevated FFA levels can be triggered by specific changes in adipose function, resulting in associated hepatic changes with minimal secondary effects in muscle. This is a key point, because muscle is the primary tissue for glucose disposal. Indeed, targeted knockout of PPARγ in muscle results in profound IR in muscle (31). Ongoing studies in adipose/muscle double-KO mice should help to further refine this hypothesis to genetically define the primary and secondary sites of syndrome X and the pathophysiology of type II diabetes.

We thank Dr. S. O'Gorman (Case Western Reserve University, Cleveland) for Cre cDNA plasmid; Dr. P. Tontonoz (University of California, Los Angeles) for mouse aP2 enhancer/promoter genomic DNA plasmid; Drs. R. Yu, Y. Wang, C. Lee, and J. Rosenfeld for critical reading and discussion of the manuscript; J. Arimura for technical help and animal care; and E. Stevens and B. Hansen for preparation of the manuscript. R.M.E. is an investigator of the Howard Hughes Medical Institute and March of Dimes Chair in Molecular and Developmental Biology at the Salk Institute. This study was supported by National Institutes of Health Grants DK-33651 (to J.M.O.), DK-60484 (to A.H.), 2T32 DK07044-23 and NIHDK07494 (to W.H.), and DK57978-24 (to R.M.E.); the National Institute for Diabetes and Digestive and Kidney Diseases; National Heart, Lung, and Blood Institute Grant HL56989 (to R.M.E.); the Hilblom Foundation (J.M.O. and R.M.E.); and the Department of Veterans Affairs Research Service.

1. Spiegelman, B. M. (1998) *Diabetes* **47,** 507–514.
2. Barroso, I., Gurnell, M., Crowley, V. E., Agostini, M., Schwabe, J. W., Soos, M. A., Maslen, G. L., Williams, T. D., Lewis, H., Schafer, A. J., *et al*. (1999) *Nature* **402,** 880–883.
3. Lehmann, J. M., Moore, L. B., Smith-Oliver, T. A., Wilkison, W. O., Willson, T. M. & Kliewer, S. A. (1995) *J. Biol. Chem.* **270,** 12953–12956.
4. Tontonoz, P., Hu, E. & Spiegelman, B. M. (1994) *Cell* **79,** 1147–1156.
5. Okuno, A., Tamemoto, H., Tobe, K., Ueki, K., Mori, Y., Iwamoto, K., Umesono, K., Akanuma, Y., Fujiwara, T., Horikoshi, H., *et al*. (1998) *J. Clin. Invest.* **101,** 1354–1361.
6. Lee, M. K., Miles, P. D., Khoursheed, M., Gao, K. M., Moossa, A. R. & Olefsky, J. M. (1994) *Diabetes* **43,** 1435–1439.
7. Nolan, J. J., Ludvik, B., Beerdsen, P., Joyce, M. & Olefsky, J. (1994) *N. Engl. J. Med.* **331,** 1188–1193.
8. Olefsky, J. M. (2000) *J. Clin. Invest.* **106,** 467–472.
9. Spiegelman, B. M. & Flier, J. S. (1996) *Cell* **87,** 377–389.
10. Deeb, S. S., Fajas, L., Nemoto, M., Pihlajamaki, J., Mykkanen, L., Kuusisto, J., Laakso, M., Fujimoto, W. & Auwerx, J. (1998) *Nat. Genet.* **20,** 284–287.
11. Kubota, N., Terauchi, Y., Miki, H., Tamemoto, H., Yamauchi, T., Komeda, K., Satoh, S., Nakano, R., Ishii, C., Sugiyama, T., *et al*. (1999) *Mol. Cell* **4,** 597–609.
12. Miles, P. D., Barak, Y., He, W., Evans, R. M. & Olefsky, J. M. (2000) *J. Clin. Invest.* **105,** 287–292.
13. Magre, J., Delepine, M., Khallouf, E., Gedde-Dahi, T., Jr., Van Maldergem, L., Sobel, E., Papp, J., Meier, M., Megarbane, A., BSCL Working Group, *et al*. (2001) *Nat. Genet.* **28,** 365–370.
14. Moitra, J., Mason, M. M., Olive, M., Krylov, D., Gavrilova, O., Marcus-Samuels, B., Feigenbaum, L., Lee, E., Aoyama, T., Eckhaus, M., *et al*. (1998) *Genes Dev.* **12,** 3168–3181.
15. Shimomura, I., Hammer, R. E., Richardson, J. A., Ikemoto, S., Bashmakov, Y., Goldstein, J. L. & Brown, M. S. (1998) *Genes Dev.* **12,** 3182–3194.
16. Chao, L., Marcus-Samuels, B., Mason, M. M., Moitra, J., Vinson, C., Arioglu, E., Gavrilova, O. & Reitman, M. L. (2000) *J. Clin. Invest.* **106,** 1221–1228.
17. Gavrilova, O., Marcus-Samuels, B., Graham, D., Kim, J. K., Shulman, G. I., Castle, A. L., Vinson, C., Eckhaus, M. & Reitman, M. L. (2000) *J. Clin. Invest.* **105,** 271–278.
18. Gu, H., Zou, Y. R. & Rajewsky, K. (1993) *Cell* **73,** 1155–1164.
19. Zhu, Y., Qi, C., Korenberg, J. R., Chen, X. N., Noya, D., Rao, M. S. & Reddy, J. K. (1995) *Proc. Natl. Acad. Sci. USA* **92,** 7921–7925.
20. Barak, Y., Liao, D., He, W., Ong, E. S., Nelson, M. C., Olefsky, J. M., Boland, R. & Evans, R. M. (2002) *Proc. Natl. Acad. Sci. USA* **99,** 303–308.
21. Soriano, P. (1999) *Nat. Genet.* **21,** 70–71.
22. O'Brien, S. N., Mantzke, K. A., Kilgore, M. W. & Price, T. M. (1996) *Anal. Quant. Cytol. Histol.* **18,** 137–143.
23. Kelly, L. J., Vicario, P. P., Thompson, M., Candelore, M. R., Doebber, T. W., Ventre, J., Wu, M. S., Meurer, R., Forrest, M. J., Conner, M. W., *et al*. (1998) *Endocrinology* **139,** 4920–4927.
24. Barak, Y., Nelson, M. C., Ong, E. S., Jones, Y. Z., Ruiz-Lozano, P., Chien, K. R., Koder, A. & Evans, R. M. (1999) *Mol. Cell* **4,** 585–595.
25. Ravussin, E. & Smith, S. R. (2002) *Ann. N.Y. Acad. Sci.* **967,** 363–378.
26. Petersen, K. F., Befroy, D., Dufour, S., Dziura, J., Ariyan, C., Rothman, D. L., DiPietro, L., Cline, G. W. & Shulman, G. I. (2003) *Science* **300,** 1140–1142.
27. Berg, A. H., Combs, T. P., Du, X., Brownlee, M. & Scherer, P. E. (2001) *Nat. Med.* **7,** 947–953.
28. Combs, T. P., Berg, A. H., Obici, S., Scherer, P. E. & Rossetti, L. (2001) *J. Clin. Invest.* **108,** 1875–1881.
29. Yamauchi, T., Kamon, J., Waki, H., Terauchi, Y., Kubota, N., Hara, K., Mori, Y., Ide, T., Murakami, K., Tsuboyama-Kasaoka, N., *et al*. (2001) *Nat. Med.* **7,** 941–946.
30. Combs, T. P., Wagner, J. A., Berger, J., Doebber, T., Wang, W. J., Zhang, B. B., Tanen, M., Berg, A. H., O'Rahilly, S., Savage, D. B., *et al*. (2002) *Endocrinology* **143,** 998–1007.
31. Hevener, A. L., He, W. M., Barak, Y., Le, J., Bandyopadhyay, G., Olson, P., Wilkes, J., Evans, R. M. & Olefsky, J. M. (2003) *Nat. Med.* **9,** 1491–1497.